Psychophysiology, *49* (2012), 43–55. Wiley Periodicals, Inc. Printed in the USA.

DOI: 10.1111/j.1469-8986.2011.01270.x

Alpha modulation in parietal and retrosplenial cortex correlates with navigation performance

TE-CHENG CHIU,[a,b] KLAUS GRAMANN,[a,c] LI-WEI KO,[a,d] JENG-REN DUANN,[a,e] TZYY-PING JUNG,[a,c] AND CHIN-TENG LIN[a,b]

[a]Brain Research Center, University System of Taiwan, Hsinchu, Taiwan
[b]Department of Computer Science, National Chiao-Tung University, Hsinchu, Taiwan
[c]Swartz Center for Computational Neuroscience, University of California San Diego, San Diego, California, USA
[d]Department of Biological Science and Technology, National Chiao-Tung University, Hsinchu, Taiwan
[e]Biomedical Engineering Research Center, China Medical University Hospital, Taichung, Taiwian

Abstract

The present study investigated the brain dynamics accompanying spatial navigation based on distinct reference frames. Participants preferentially using an allocentric or an egocentric reference frame navigated through virtual tunnels and reported their homing direction at the end of each trial based on their spatial representation of the passage. Task-related electroencephalographic (EEG) dynamics were analyzed based on independent component analysis (ICA) and subsequent clustering of independent components. Parietal alpha desynchronization during encoding of spatial information predicted homing performance for participants using an egocentric reference frame. In contrast, retrosplenial and occipital alpha desynchronization during retrieval covaried with homing performance of participants using an allocentric reference frame. These results support the assumption of distinct neural networks underlying the computation of distinct reference frames and reveal a direct relationship of alpha modulation in parietal and retrosplenial areas with encoding and retrieval of spatial information for homing behavior.

Descriptors: Spatial navigation, Allocentric, Egocentric, Reference frame, Electroencephalography (EEG), ICA

Spatial orientation is a complex cognitive task frequently occurring in our daily life during way-finding or environment exploration. Various strategies, such as path integration and piloting, can be used to compute position and to maintain orientation (Loomis, Klatzky, Golledge, & Philbeck, 1999). Irrespective of the strategy used, however, a spatial representation of the environment has to be computed, integrating the position of the navigator and other entities in the environment as well as action plans. Two classes of spatial representation systems are generally employed: one based on an allocentric reference frame and the other based on an egocentric reference frame (Klatzky, 1998). In the egocentric reference frame, the spatial location of an object is specified with respect to the navigator. The spatial representation of an object depends on the position and orientation of the observer and changes according to navigator movements. In contrast, the allocentric spatial location of an object is defined by its relationship to other objects independent of the orientation of the navigator. Individuals who prefer using an allocentric reference frame describe the spatial location of an object with respect to the features of an environment.

Spatial orientation is based on a combination of cognitive functions that are associated with activations in the frontal, parietal, premotor, occipital, and temporal cortices (Ekstrom et al., 2003; Gron, Wunderlich, Spitzer, Tomczak, & Riepe, 2000; Maguire et al., 1998; Shelton & Gabrieli, 2002). Several studies have demonstrated the importance of the parietal region in maintaining orientation based on an egocentric reference frame (Karnath, 1997; Thut, Nietzel, & Pascual-Leone, 2005). Place cells, located in the hippocampus of rodents and humans, were shown to play an important role for the computation of a cognitive map of the environment based on an allocentric

This work was supported in part by the Aiming for the Top University Plan of National Chiao Tung University, the Ministry of Education, Taiwan, and by the UST-UCSD International Center of Excellence in Advanced Bioengineering sponsored by the Taiwan National Science Council I-RiCE Program under Grant Number: NSC-99-2911-I-009-101. This research was also sponsored in part by the Army Research Laboratory and was accomplished under Cooperative Agreement Number W911NF-10-2-0022. The views and the conclusions contained in this document are those of the authors and should not be interpreted as representing the official policies, either expressed or implied, of the Army Research Laboratory or the U.S. Government. The U.S. Government is authorized to reproduce and distribute reprints for Government purposes notwithstanding any copyright notation herein. The first and second authors contributed equally to the manuscript.

Address correspondence to: Chin-Teng Lin, Ph.D., Brain Research Center, National Chiao-Tung University (NCTU), 1001 Ta-Hsueh Road, Hsinchu, Taiwan 300, ROC. E-mail: ctlin@mail.nctu.edu.tw

PSYCHOPHYSIOLOGY

reference frame (Doeller, Barry, & Burgess, 2010; Ekstrom et al., 2003; Maguire, 1997; Maguire et al., 1998; O'Keefe & Dostrovsky, 1971). Moreover, lesions in the parietal and hippocampal cortices are accompanied by impaired spatial navigation behavior (Gilbert, Kesner, & DeCoteau, 1998; Maguire, Nannery, & Spiers, 2006; Moscovitch, Nadel, Winocur, Gilboa, & Rosenbaum, 2006; Moscovitch et al., 2005; Rosenbaum et al., 2000; Seubert, Humphreys, Muller, & Gramann, 2008). These results and other neuropsychological studies suggest a functional dissociation between the use of an allocentric and an egocentric reference frame (Fink et al., 2003; Seubert, Humphreys, Muller, & Gramann, 2008; Vallar et al., 1999). Further support for a functional dissociation has come from imaging studies demonstrating different networks to support the use of distinct reference frames. While a fronto-premotor-parietal network is involved in processing egocentric information (Committeri et al., 2004; Galati et al., 2000; Gramann, Muller, Schonebeck, & Debus, 2006; Mellet et al., 2000; Zaehle et al., 2007), a network comprising the parietal cortex, occipito-temporal areas including the parahippocampal region, the hippocampus, and thalamus is involved in encoding allocentric spatial information (Gramann et al., 2006; Gron et al., 2000; Jordan, Schadow, Wuestenberg, Heinze, & Jancke, 2004; Shelton & Gabrieli, 2002; Zaehle et al., 2007).

Electroencephalographic (EEG) studies have further demonstrated that visuospatial navigation tasks are associated with modulations of specific frequency bands (Buzsaki, 2005; Caplan, Madsen, Raghavachari, & Kahana, 2001; Caplan et al., 2003; Gramann et al., 2010; Kahana, Sekuler, Caplan, Kirschen, & Madsen, 1999; Raghavachari et al., 2001). For example, alpha-band (8–12 Hz) modulation has been shown to be more pronounced during navigation in complex mazes as compared to simple mazes (Caplan et al., 2001) and to be more attenuated during heading changes as compared to simple translations (Gramann et al., 2010). Other studies, particularly investigations analyzing cortical (ECoG) signals, have found task-dependent theta (4–7 Hz) synchronization in several cortical areas including temporal, frontal, and parietal regions during spatial navigation (Caplan et al., 2001, 2003; Ekstrom et al., 2003, 2005; Kahana et al., 1999). However, none of these studies tested for the association of distinct reference frames with spectral modulation in specific frequency bands during navigation.

Gramann and colleagues (2010) recently described modulations in distinct frequency bands in distinct cortical networks to be dependent on the reference frame participants used during spatial navigation through virtual tunnels. The use of an egocentric reference frame was associated with increased alpha suppression in or near primary visual cortex while the use of an allocentric reference frame was associated with alpha attenuation in or near bilateral secondary visual cortex, bilateral inferior parietal cortex, and in or near the retrosplenial cortex (Gramann et al., 2010). In this study, participants reacted to a homing challenge based on a 2-alternative forced choice task. As a consequence, no measures of homing accuracy were recorded and analyzed with respect to the accompanying brain dynamics. The present study investigated the EEG dynamics of participants using an egocentric or an allocentric reference frame to test whether specific frequencies in distinct regions of the brain are associated with spatial orienting behavior on a trial-to-trial basis. To this end, we adapted the tunnel task used in earlier studies to a three dimensional (3D) virtual reality, driving-simulation environment where subjects actively indicated the origin of the passage after each trial.

Materials and Methods

Experimental Paradigm

Participants performed a tunnel task in a virtual reality (VR) based driving environment while sitting comfortably in a real car (without the unnecessary weight of the engine and other components) mounted on the center of a Stewart motion platform (Hsu et al., 2005) circularly surrounded by six projection screens. The surrounding screens provided a 206° frontal and 40° back field view during virtual driving. The virtual realistic tunnel scenery was constructed with the WorldToolKit (WTK) library (SENSE8, Mill Valley, CA).

The tunnel task consisted of an encoding phase and a retrieval phase. Participants traversed through virtual tunnels with a turn to the left or the right (encoding phase) and subsequently were asked to point to the origin of the passage (retrieval phase; see Figure 1A). In earlier studies using the tunnel task, navigation times were held constant for different tunnel trials resulting in higher angular velocities with increasingly acute angles of the turn. In the present study, angular velocity was kept constant for all tunnels resulting in a constant optical flow independent of the angle of heading changes.

Participants were asked to keep up orientation during tunnel passages and to adjust a 3D homing arrow at the end of each trial. During the encoding phase, animations of passages through a virtual tunnel were presented on the screen simulating a car driving with constant velocity at about 46 km/h. Participants perceived sparse visual flow of a virtual tunnel beginning with a 2.4 s straight tunnel segment followed by a 3.8–8 s turning segment with the duration of heading changes dependent on the angle of the turn (see Figure 1B). All tunnels included only one turn of varying angle (degree of turns 15°, 30°, and 45°) randomly to the left or the right. The VR scene provided participants with visual flow of spatial translation and rotation only. No motion was provided via the platform. There were no landmarks or reference points in the tunnel scenery.

The retrieval phase started after the tunnel passage ended. First, participants were required to indicate the homing direction by selecting whether it was to their 'right rear' or 'left rear.' A 3D homing arrow was projected on the screen, and participants had to press the left or right button on the steering wheel to indicate that the origin of the passage was behind them and to their left or to their right, respectively. This selection was used to determine the preferred strategy of the participant (a response based on an allocentric or an egocentric reference frame). Participants were selected for further analyses only if they used an identical strategy on 90% or more of all trials. For a tunnel with a turn to the right, participants using an allocentric reference frame would indicate that the starting point was behind them and to their left (see Figure 1C). Participants reacting based on an allocentric reference frame are named 'Nonturner' in the remainder of this document. In contrast, participants using an egocentric reference frame would report that the origin was behind them and to their right. Participants reacting based on an egocentric reference frame are labelled 'Turner' for the remainder of this document. Please note that the labels do not describe individual traits but rather spatial strategies by using one or the other or a combination of reference frames (Gramann, in press). After indicating the general homing direction, participants were asked to indicate the correct homing angle. Once participants confirmed the binary homing selection by pressing the respective button, the homing arrow started to rotate to the indicated direction and participants

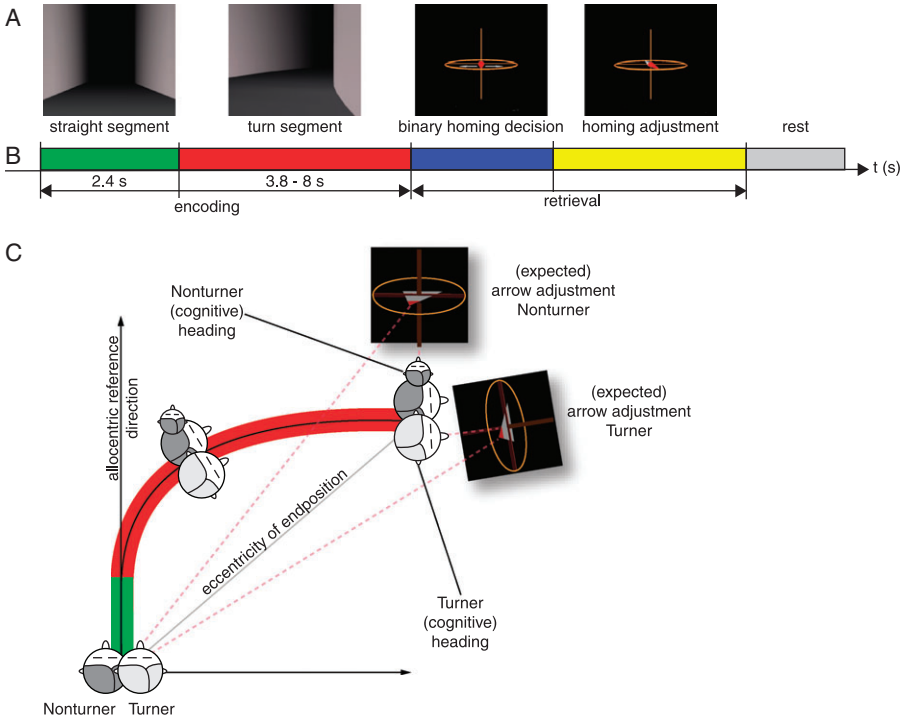

Figure 1. Experimental design. (A) Screenshots of the virtual-reality tunnel and homing arrows for participants to point back to their origins before the turns. (B) The time line of one tunnel trial composed of an encoding phase (green and red colored time periods) and a retrieval phase (blue and yellow colored time periods) and subsequent rest before the next trial (gray time period). During the encoding phase, participants were asked to keep up orientation. At the end of the tunnel, an arrow would direct participants to decide the direction toward the starting point (binary homing decision, blue colored time period). Then, the arrow started to rotate from the middle to the selected direction at an angular velocity of 10° per second. Participants were asked to press a button to stop the rotating arrow when they thought the pointing direction of the arrow exactly pointed to the homing direction (yellow colored time period). (C) Cartoon heads of Nonturners (dark gray head) and Turners (light gray head) represent the cognitive heading of both strategy groups during a tunnel passage with a turn to the right. The first straight segment and the following turn are marked green and red according to the phases described in (B). The homing arrows at the end of the passage represent the homing direction based on the cognitive heading of subjects at the end of the passage. Note that for tunnels with one turn (to the right in this figure) the homing directions differ for Turners and Nonturners with the former strategy group pointing back and to their right and the latter strategy group pointing back and to their left.

had to press the button again to stop the rotation of the arrow when it reached the desired homing angle. Participants were asked to practice the task for at least 5 min until they were familiar with it. Subsequently, each participant was required to complete four 20-min sessions in the experiment with each session containing 45 trials. Between sessions, participants could take a break for about 5–10 min. The experiment was recorded by a video camera for monitoring and evaluating the behavior of participants.

Participants

Twenty right-handed participants were paid to take part in the tunnel experiment (age: 21–30 years, mean = 24.8, $SD = 2.76$ years, 7 females). None of the participants had a history of neurological or psychiatric disorders or a history of drug or alcohol abuse. None of the participants reported sleep deprivation the night before performing the experiment. All participants had normal or corrected-to-normal vision and were not aware of the hypotheses at the time of testing. They gave their written informed consent to the procedure, which was approved by the Institutional Review Board of Taipei Veterans General Hospital. Ten of the participants were categorized as Nonturners (using an allocentric reference frame; 8 male, 2 female) and 7 were categorized as Turners (using an egocentric reference frame; 3 male, 4 female). The remaining 3 participants could not be classified unambiguously because their homing responses were based on distinct reference frames in more than 10% of all trials (mean consistency = 60%, $SD = 7.9\%$).

Signal Acquisition

Physiological data were recorded using 32 unipolar sintered Ag/AgCl electrodes. All electrodes were placed in an elastic cap according to a subset of a 10% system (Fp1, Fp2, Fz, F3, F4, F7, F8, FCz, FC3, FC4, FT7, FT8, Cz, C3, C4, CPz, CP3, CP4, Pz, P3, P4, T3, T4, T5, T6, TP7, TP8, Oz, O1, O2, A1, A2) with impedances kept below 5 kΩ. EEG data were recorded with the Scan NuAmps Express system (Compumedics Ltd., Victoria, Australia) and digitized at 1000 Hz and 16-bit quantization precision. The absolute electrode 3D positions were recorded for each participant with a digitizer system.

Data Processing

Participants were first classified as Nonturner or Turner based on their homing responses at the end of the tunnel passages. In contrast to earlier studies, the categorization was based on the

binary question of homing direction (left or right) as part of the experimental trials and not during an additional *a priori* categorization task (Gramann, Muller, Eick, & Schonebeck, 2005). Subsequently, participants were asked to indicate the homing angle by stopping the subsequent rotation of the same 3D homing arrow. To investigate the difference in task performance between participants using an egocentric or an allocentric reference frame, response times (the time participants needed to indicate the initial homing direction), and mean homing error (of the subsequent homing adjustment) were analyzed. Trials with turns to the left were merged with right-turn trials after trials with homing errors exceeding three times the standard deviation of the individual mean error were removed as outliers. A 2×3 mixed design analysis of variance (ANOVA) with the between-subject factor 'strategy' (Nonturner vs. Turner) and the repeated measures factor turning 'angle' (15°, 30°, 45°) were used to analyze task performance.

The continuous EEG signals were analyzed using MATLAB (The Mathworks, Inc.) and the open source toolbox EEGLAB (http://sccn.ucsd.edu/eeglab). EEG signals were first downsampled to 250 Hz and filtered using a low-pass filter with a cut-off frequency of 50 Hz and a high-pass filter with a cut-off frequency of 0.5 Hz (stop-band attenuation of 20 dB). These filter settings were chosen to replicate those of a previous investigation (Gramann et al., 2010) with a low-pass filter attenuating line noise and a high-pass filter improving decomposition by means of independent component analysis (ICA) due to the elimination of nonstationarity in the signal. Signal intervals containing electrode noise or large bursts of muscle artifacts were identified by visual inspection using the EEGLAB visualization tool and eliminated before further processing. The mean number of remaining trials per participant was 168.8 ($SD = 22.5$).

ICA and component selection. ICA has been extensively applied to blind source separation problems, and it has been shown that ICA is a suitable solution to the problem of segregation of statistically independent time sources and their subsequent localization in a biophysical source space (Jung et al., 2000, 2001; Lee, Girolami, & Sejnowski, 1999; Makeig, Debener, Onton, & Delorme, 2004; Makeig, Gramann, Jung, Sejnowski, & Poizner, 2009; Makeig, Jung, Bell, Ghahremani, & Sejnowski, 1997; Onton, Westerfield, Townsend, & Makeig, 2006). The 'runica' procedure in EEGLAB was applied to decompose EEG signals into statistically maximally independent components (ICs). The initial learning rate was set to 10E-4; training was stopped when the learning rate (a unitless scaling factor) fell below 10E-6. An equivalent current dipole model was then computed for each IC by using DIPFIT2 routines from EEGLAB. To this end, a four-shell spherical head model (Oostenveld & Oostendorp, 2002) with default radii values for the four spheres (71, 72, 79, and 85 mm) and the default conductance values (0.33, 1.0, 0.0042, and 0.33 S/m) were used to compute the approximate location of each equivalent dipole source. Because of the dipolarity of the scalp maps associated with each IC representing the strength of the volume-conducted component activity at each scalp electrode (Makeig et al., 2004), each scalp map can be approximated using a single (or, in the case of a dual dipolar scalp map, a dual) dipole solution without any further model assumptions. For each dipolar scalp map, an equivalent dipole solution with one equivalent dipole model was computed. In case of dual dipolar scalp maps most likely representing bilateral synchronous activation (e.g., in extrastriate visual cortex), equivalent dual dipole solutions with a symmetry constraint were used. Only dipoles with a residual variance smaller than 15% that were located in the brain space of the Montreal Neurological Institute (MNI) forward solutions were selected for further analyses. This way clear dipolar solution that accounted for muscle activity of mechanical artifacts were excluded. Some ICs were identified as accounting for blinks and other eye movements, or muscle artifacts according to their scalp maps, equivalent dipole model location, and spectral profiles. ICs were selected based on the same criteria that were used in Gramann et al. (2010) as reflecting brain source activity based on their power spectrum (with a prominent peak in the frequency range from 3 to 15 Hz), their scalp maps (i.e., scalp maps had to be modeled with a single dipole or a symmetrical dual dipole solution with a residual variance of 15% or less), and the location of the equivalent dipole model computed for each IC (only equivalent dipole models that were located inside the brain were selected).

Time-frequency analysis and event-related spectral perturbation statistics. Selected components' time series during each tunnel trial were converted into spectrographic images using fast Fourier transform (FFT) in the frequency range from 3 to 50 Hz on data windows of 512 sample points that were multiplied by a gain factor determined by a Hanning window and then extended to 1024 points by zero-padding. Subsequently, event-related spectral perturbation (ERSP) images were computed by converting single trial spectrographic images to mean log power and subtracting mean log power from a baseline interval composed of straight tunnel segments (Makeig, 1993). This way, increases and decreases in spectral power during the task as compared to spectral power during a baseline condition can be displayed. Significant deviations from baseline power were assessed by bootstrapping, a nonparametric permutation-based statistical method. Nonsignificant points were masked as zero so that only significant ($p < .01$) perturbations from the baseline were color-coded (Delorme & Makeig, 2004).

The 'timewarp' procedure in EEGLAB was used to linearly transform the ERSP matrices in order to normalize the time length difference between each tunnel type (see Gwin, Gramann, Makeig, & Ferris, 2010 for time-warping to gait cycles). To this end, mean event latencies for onset of tunnel movement, onset of turning segment, offset of turning segment, and different response times were computed. Subsequently, single-trial, event-related spectral perturbation was linearly stretched or compressed to the mean event latencies of all events of interest and subsequently averaged for each participant. This allowed for a direct comparison of all trials independent from differences in event latencies.

Component clustering and cross-subject analysis. All selected ICs were clustered based on their mean IC log spectra, event-related potentials (ERPs), equivalent dipole locations, ERSP, and intertrial coherence (ITC) (Delorme & Makeig, 2004; Gramann et al., 2010; Makeig et al., 2002). First, we compressed and combined each IC measure to 10 dimensions (except dipole location with three dimensions: x, y, z) by principal component analysis (PCA) resulting in a 43-dimensional combined measure. Subsequently, we applied PCA once again to further reduce the 43-dimensional combined measure into a single 25-dimensional position vector for each IC. The 3D measure of dipole location was multiplicatively weighted by a factor of 15 to compensate for

the reduced dimensionality (three spatial dimension of x, y, and z). ERSP principal components were weighted by 3 while scalp topographies were not included. All other measures (spectrum, ERP, and intertrial coherence) were given a weight of 1. The dimensionality reduction and weight setting replicates the setting used in the Gramann et al. (2010) study. Finally, ICs were clustered by applying the *K*-means algorithm to the 25-dimensional measure clustering the data according to the distance of measures between each other in the vector space. The *K*-means method will produce clusters with the greatest possible distinction by minimizing variability within and maximizing variability between clusters. ICs with a distance larger than three standard deviations from the mean of any cluster centroid were removed from the analysis.

To further display the average ERSP of a component cluster (cross-subject ERSP), all epochs of ICs were concatenated for different clusters and subsequently normalized (zero-mean, unit standard deviation) across subjects. Statistical tests for significant differences in power perturbations were computed using bootstrapping statistics ($p < .01$). For cross-group ERSP analysis, we further computed the differences of Nonturner ERSP and Turner ERSP for each cluster and computed the significance of these differences using bootstrapping statistics ($p < .01$).

Correlation analysis. In order to investigate the relationship between brain dynamics and homing responses, we first correlated IC spectral perturbations in different frequency bands with the absolute value of the individually adjusted homing angle on single trials. A second correlation was computed for the IC spectral series in different frequency bands and the individual signed homing error. To this end, IC activations were first decomposed into time-frequency domain by short-term Fourier transform. Subsequently, the correlation between power changes in each time-frequency point and absolute adjusted homing angle was computed. Nonsignificant correlation coefficients were masked (by setting them to zero), preserving only those time-frequency points that revealed a significant correlation with the homing arrow adjustments ($p < .01$). For example, a positive correlation of homing adjustments (or relative errors in adjustment) with a specific time-frequency point indicated power increases with increasing angles of the homing adjustment (or increasing errors of the adjustment) at that specific time-frequency point. Only clusters with significant covariations of homing adjustments or errors in homing adjustments and spectral modulations in one or more different frequency bands were further investigated.

Results

Performance Measures

Average response times for Nonturners were 663.8 ms, 680.5 ms, and 643.6 ms for tunnels with 15°, 30°, and 45° turns, respectively. Turner participants showed average response times of 616.0 ms, 610.3 ms, and 624.3 ms for 15°, 30°, and 45° turns, respectively. A mixed model ANOVA with the subjects' 'Strategy' as between-subject factor and 'Angle' of heading change as repeated measure revealed no apparent differences in the distributions of response times for the two strategy groups [$F(1,15) = 0.255$, $p = .621$, $\text{eta}^2 = 0.017$]. Similarly, the angle of heading changes during the tunnel passage did not have any influences on response times [$F(2,30) = 0.45$, $p = .956$, $\text{eta}^2 = 0.003$]. No interactions were found between participants' strategy and turning angle [$F(2,30) = 0.712$, $p = .499$, $\text{eta}^2 = 0.05$].

A similar analysis for individual homing adjustments revealed angular adjustments of 20.0°, 27.4°, and 36.4° for Nonturners for tunnels with 15°, 30°, and 45° turns, respectively. Turner participants adjusted 24.3°, 30.9°, and 39.8° to point back home from the different end positions (see Figure 2A). Homing adjustments of both strategy groups were comparable [$F(1,15) = 0.762$, $p = .396$, $\text{eta}^2 = 0.048$] and no interactions were found between the strategy of the participants and turning angle [$F(2,30) = 0.293$, $p = .748$, $\text{eta}^2 = 0.003$]. Moreover, homing adjustments of both strategy groups revealed a strong tendency to overestimate homing angles when heading changes were small while underestimating homing angles when heading changes were large. Nonturners showed homing errors of 3.9°, −2.4°, and −8.1° while Turners showed errors of 12.0°, 2.7°, and −3.8° for 15°, 30°, and 45° turns, respectively (see Figure 2B). Their relative errors were comparable [$F(1,15) = 1.645$, $p = .219$, $\text{eta}^2 = 0.099$] and no interactions were found between the strategy of the participants and turning angle [$F(2,30) = 1.045$, $p = .364$, $\text{eta}^2 = 0.015$].

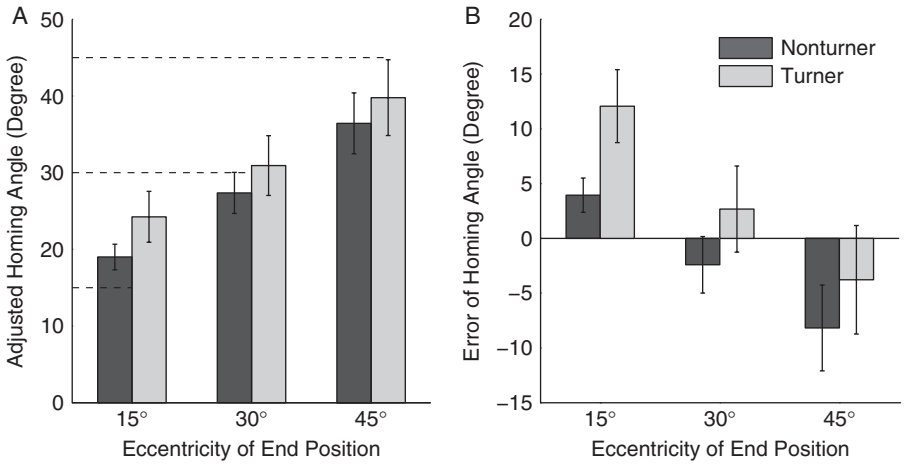

Figure 2. Homing performance of Turner and Nonturner participants. Please note that values of Turners were transformed into an allocentric reference frame to allow for direct comparison with Nonturners. (A) Homing angle reported by participants (Y-axis) as a function of turning angle (X-axis). Error bars indicate ± 1 standard error. Black dashed lines show expected homing angles for the different turning angles. (B) Signed homing error as a function of turning angle.

Component Clusters

Ten component clusters with independent component processes located in the brain were returned by *K*-means (Figure 3). Figure 3 shows equivalent dipole models representing the locations of all ten clusters of IC processes with equivalent dipole model locations in the MNI brain space and the associated scalp maps. Please note that equivalent dipole locations are only an approximation of the origin in the biophysical source space.

Of these ten component clusters, seven clusters revealed significant correlations of spectra with participants' homing arrow adjustments. These were located in or near the left inferior parietal cortex (Cls 1), the right postcentral gyrus (Cls 2), the left precuneus (Cls 3), the medial posterior cingulate cortex (Cls 4), the posterior cingulate (retrosplenial) cortex (Cls 5), and the left and right lateral occipital cortex (clusters 6 and 7, respectively). Figure 4 compares spectral characteristics of Nonturners and Turners during encoding and retrieval of the spatial information.

For Nonturners, significant ($p < .01$) power decreases in the alpha and beta bands were observed in or near the left inferior parietal and right post-central cortex, as well as the left precuneus (see Figure 4A, Cls 1, 2, and 3) during encoding and retrieval of spatial information (indicated by the solid square exemplarily in Cls 1). This desynchronization of alpha and beta was accompanied by a significant increase in power for frequencies between 15 and 20 Hz (indicated by the broken square in Cls 1) in or near the left inferior parietal cortex and the right post-central cortex (Cls 1 and 2, respectively) but not in or near the left precuneus (Cls 3). In both posterior cingulate cortex clusters (Cls 4 and 5), the alpha as well as the beta band of Nonturners synchronized approaching the end of the turning section, persisting through the binary homing decision (indicated by the broken square in Cls 4). This power increase was immediately followed by strong desynchronization that lasted over the entire time window of the homing arrow adjustment (solid square in Cls 4). Power modulation in or near the lateral occipital region (see Figure 4A, Cls 6 and 7) was comparable to power changes in or near the posterior cingulate cortex but appeared to include wider frequency bands. A strong synchronization in the alpha and beta band was revealed at the end of the turning section, persisting through the binary homing decision. We found a wide bandwidth (from 6 to 18 Hz) of desynchronization in the alpha band in the lateral occipital cortex. Compared to Turner participants, Nonturners demonstrated pronounced desynchronization of the alpha frequency bands in both posterior cingulate cortex (Cls 4 and 5) and occipitals clusters (Cls 6 and 7), particularly during the recall phase.

Turner participants demonstrated significant ($p < .01$) alpha (8–12 Hz) and beta (20–30 Hz) band power modulation in component clusters with centroids located in or near the left precuneus (Cls 3) and left inferior parietal, as well as the right post-central cortices (Cls 1 and 2) during all phases of spatial navigation (see Figure 4B, area marked by solid square). This power attenuation was observed during encoding, shifted to a slightly higher frequency band and increased with onset of the

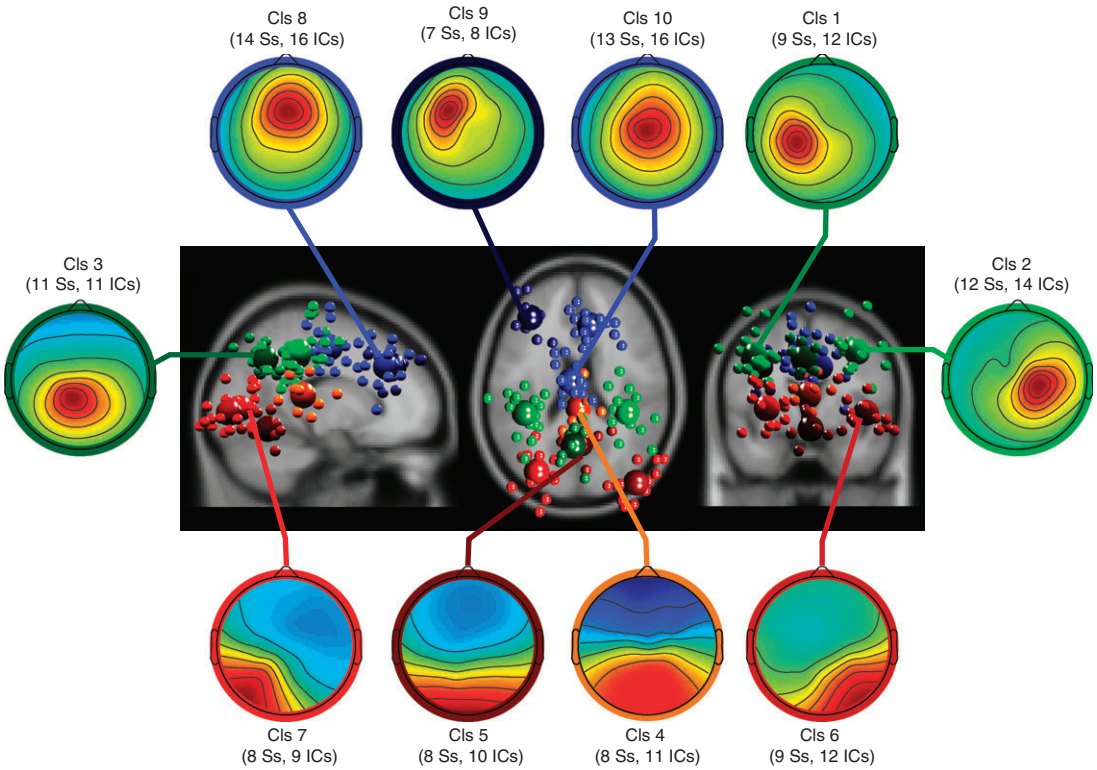

Figure 3. Clusters of independent component processes projected to the standard brain with small spheres representing individual equivalent dipole models and big spheres representing the centroids of the respective clusters. Different clusters with equivalent dipole models of cluster centroids located in the inner shell of the dipole model are coded with different colors (red to blue). Each cluster is connected to its respective scalp projection displayed on the surrounding of the central dipole plot. For each cluster, the number of subjects and the number of ICs is given. Cluster centroids are located in or near the left inferior parietal cortex (Cls 1), right postcentral gyrus (Cls 2), the left precuneus (Cls 3), posterior cingulate (Cls 4), posterior cingulate (Cls 5), right middle occipital gyrus (Cls 6), left middle occipital gyrus (Cls 7).

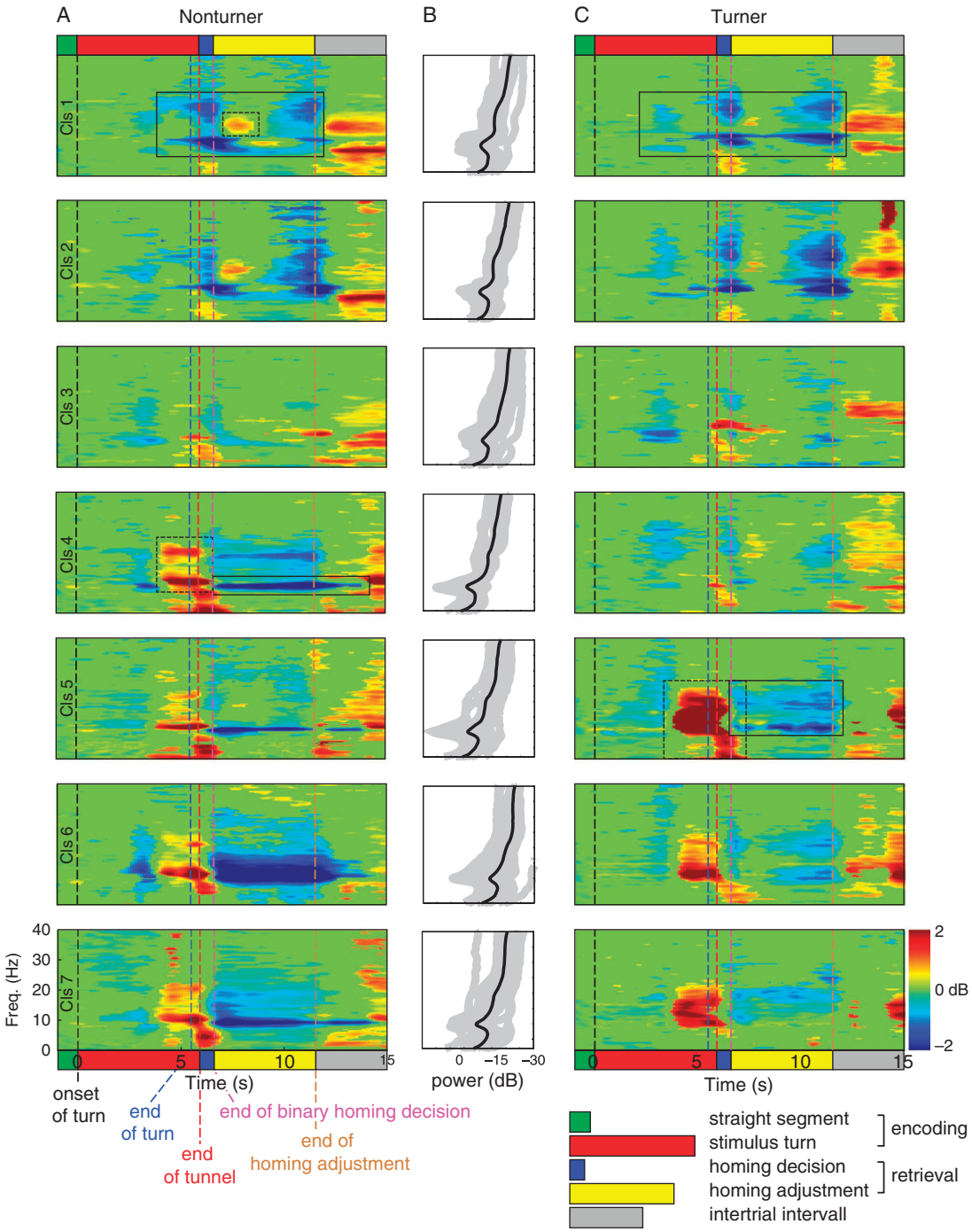

Figure 4. Event-related spectral perturbation (ERSP) for selected clusters. (A) Nonturners' ERSPs during tunnel passages from top to bottom for different clusters (as described in Figure 3). (B) Middle column shows selected cluster spectra for individual IC (light gray) and the resultant mean spectrum (black). (C) Right column displays ERSPs for Turners during tunnel passages (same clusters as described for Nonturners). Solid black outlines and broken black outlines indicate significant power decreases and increases, respectively, as discussed in the text.

binary homing decision, persisting through the end of the adjustment phase. This pattern was observed in clusters with their centroids located in or near the inferior parietal and post-central cortex (Cls 1 and 2) but not the superior parietal cortex (Cls 3). In the more ventrally located posterior cingulate cluster (Figure 4B, Cls 5), a strong synchronization in a broad frequency band from 10 to 20 Hz was observed towards the end of the encoding phase (marked with broken square) accompanied by a significant increase in the theta power during the binary homing decision. The retrieval of spatial information during the adjustment phase was then accompanied by desynchronization in the alpha and beta frequency bands for Turners (solid square). A comparable pattern of desynchronizations and synchronizations was observed in the lateral occipital cortices for Turners (see Figure 4B, Cls 6 and 7).

Correlation between EEG Dynamics and Homing Arrow Adjustments

The modulation of task-dependent brain dynamics of the seven selected component clusters with respect to the homing arrow adjustments at the end of the passage were markedly different for Turners and Nonturners (see Figure 5).

Figure 5 shows the significant correlations ($p < .01$) of time-frequency points with participants' homing adjustments. Not all frequency modulations correlated with participants' homing adjustments. A linear relationship between changes in brain dynamics and homing angle adjustments was revealed for Turners in the three parietal clusters (Cls 1, 2, and 3) for both the encoding and the recall phase (see Figure 5C, rows 1 to 3). A sustained negative correlation of homing adjustments and 10/20 Hz frequency modulation was found for the left precuneus (see Figure 5C, Cls 3 marked with black rectangles). A comparable pattern of covariation but to a lesser extent was observed in or

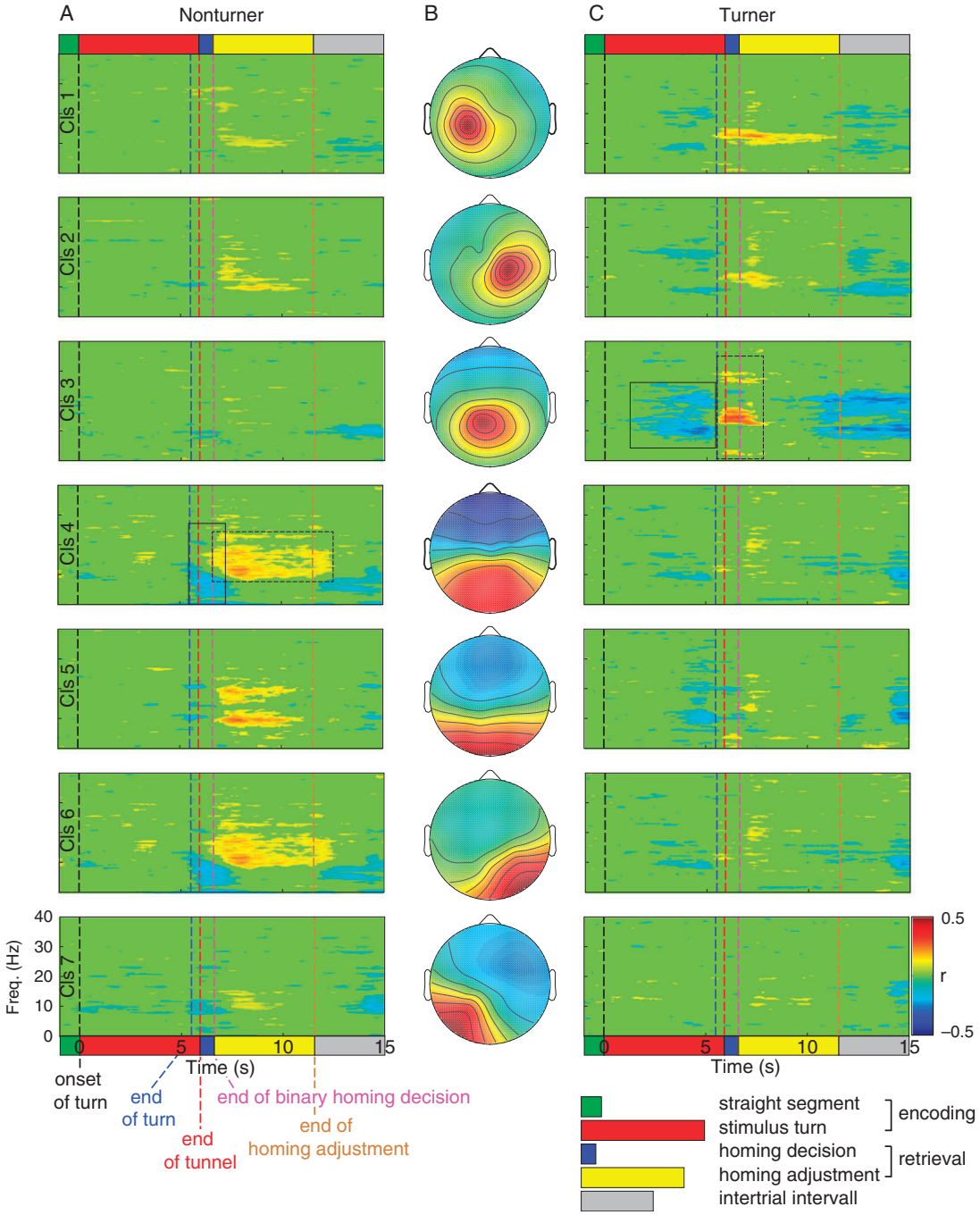

Figure 5. Correlation coefficients computed between event-related spectral perturbations (ERSP) and homing adjustments for selected clusters. (A) Nonturners' correlation of ERSPs with homing adjustment for selected clusters (as described in Figure 3). (B) Middle column shows selected cluster centroid topographic images (as in Figure 3). (C) Right column displays correlation coefficients for Turners during tunnel passages (same clusters as described for Nonturners). Solid black outlines and broken black outlines indicate significant positive and negative correlation coefficients, respectively, as discussed in the text.

near the bilateral inferior parietal cortex (see Figure 5C, Cls 1 and 2). With onset of the binary homing question, a positive correlation between power spectra of 10 to 20 Hz and homing angle adjustments was observed for Turners (marked with broken black rectangle). In addition, changes in beta-band power during the binary homing direction decision were positively correlated with homing adjustments. For Nonturners, no significant relationship between specific frequency bands and homing angle adjustments was found during the encoding phase. In contrast, a strong negative correlation was observed for power modulations in the frequency range from 5 to 10 Hz with onset of the binary homing decision in or near the posterior cingulate and occipital cortex (see Figure 5A, Cls 4, 5, 6, and 7; area of interest is marked exemplarily for all clusters in Cls 4). This was followed by a positive correlation of homing adjustments with frequencies in 10/20 Hz in both the occipital and the retrosplenial cortices during the retrieval phase.

Correlation between EEG Dynamics and Relative Error

Linear relationships between changes in brain dynamics and relative errors in participants' responses resembled the results revealed for homing adjustments in all brain regions except the posterior cingulate cortex (see Figure 6, Cls 4). Turners revealed significant negative correlations of time-frequency modulation and homing errors in or near the parietal cortex during encoding of heading changes (see Figure 6C, row 3, Cls 3; area of interest is marked with a black rectangle). This negative covariation was pronounced for the IC cluster located in or near the superior parietal cortex (Cls 3). This pattern in parietal cortices was not observed for Nonturners who revealed significant positive correlation in the alpha frequency range with homing errors only during the retrieval phase. Nonturners showed negative correlations with the onset of the binary homing decision and a positive correlation of homing adjustments in or near the posterior cingulate and right occipital cortex (see Figure 6A, Cls 5 and 6).

The retrosplenial cortex (Cls 5) showed significant correlations in both Turners and Nonturners. Nonturners revealed negative correlations of homing errors and narrow-band frequencies most pronounced around 10 Hz followed by a subsequent positive correlation of homing errors and the 10 Hz and first harmonic frequency band during retrieval of spatial information (Cls 5, indicated by the broken rectangle). Turners, in contrast, demonstrated a strong negative relationship between alpha modulation and homing errors towards the end of heading changes in or near the dorsal posterior cingulate cortex (Cls 5) but no positive correlation between alpha power and homing error during retrieval.

Discussion

This investigation used a virtual path integration task to explore the brain dynamics associated with the use of allocentric and egocentric reference frames during navigation and the subsequent retrieval of information from the resultant spatial representation. We identified neural activation patterns in a widespread posterior network associated with navigating through virtual tunnels, replicating the results from earlier studies (Gramann et al., 2010; Plank, Müller, Onton, Makeig, & Gramann, 2010). This study decomposed EEG, the surface measured linear mixture of cortical source activity, by means of ICA and subsequent localization of sources in the biophysical source space (the head model). Applied to EEG data, ICA reveals *what* distinct, e.g., temporally independent activities compose the observed scalp recordings, separating this question from the question of *where* exactly in the brain these activities arise. Although ICA does not solve the source-localization problem directly, rendering the scalp projection of the component can facilitate answers to the problem. This study approximately modeled the source distribution of each component using a single (or, in the case of a dual dipolar scalp map, a dual) dipole solution. However, this estimation of dipole location was far from precise and caused noticeable deviations in the source localization results across different subjects. The reasons are listed as follows. First, since the dipole localization results were based on only 32 scalp channels, estimation error was inevitable in such a low-density montage. Second, due to lack of precise 3D sensor locations and anatomical images from each individual, using standard sensor locations and anatomical templates probably increased errors in source locations. Therefore, the 3D equivalent dipole models reported in this study give only the approximate source locations of the involved cortical source patches (Chen et al., 2010; Lin et al., 2009).

Behavioral results replicated differences in homing adjustments with angular reactions being mirror images for the two strategy groups. During the first straight segment of a passage, both the egocentric and the allocentric reference frames are aligned. This alignment was associated with identical perceived and cognitive headings for Turner and Nonturner participants. During a turn, however, the egocentric and allocentric reference frames and consequently the cognitive headings of the two strategy groups became misaligned, while the perceptual heading (visual flow) remained the same for both groups. Turners updated their cognitive heading according to the perceived heading changes during a turn. In contrast, Nonturners computed and maintained a cognitive heading that was aligned with the initial straight segment as previously demonstrated (Gramann, El Sharkawy, & Deubel, 2009; Gramann et al., 2005, 2006, 2010). Responses of participants revealed comparably accurate homing adjustments for Turners and Nonturners based on their preferred reference frames. Both strategy groups overestimated the homing angle when turning angles were small (15°) and underestimated homing angles when turning angles were large (45°). This tendency towards the middle replicated previous findings (Gramann et al., 2005, 2010; Plank et al., 2010).

Spectral Modulations during Encoding of Spatial Information

The present study found performance-related spectral perturbations in or near superior parietal, inferior parietal, retrosplenial, and occipital cortex. These power modulations differed between the encoding and the retrieval of spatial information. This difference likely reflects activity in distinct neuronal networks associated with encoding of spatial information and retrieval of the same from a mental representation. During encoding, parietal and retrosplenial alpha power correlated with subsequent homing adjustments in Turners. The parietal cortex as part of the dorsal pathway is known to be associated with the computation and maintenance of egocentric representations (Committeri et al., 2004; Sdoia, Couyoumdjian, & Ferlazzo, 2004) as well as heading estimations (Peuskens, Sunaert, Dupont, Van Hecke, & Orban, 2001). Turners, preferentially using an egocentric reference frame, demonstrated a significant power decrease in the alpha frequency band in clusters with centroids located in or near

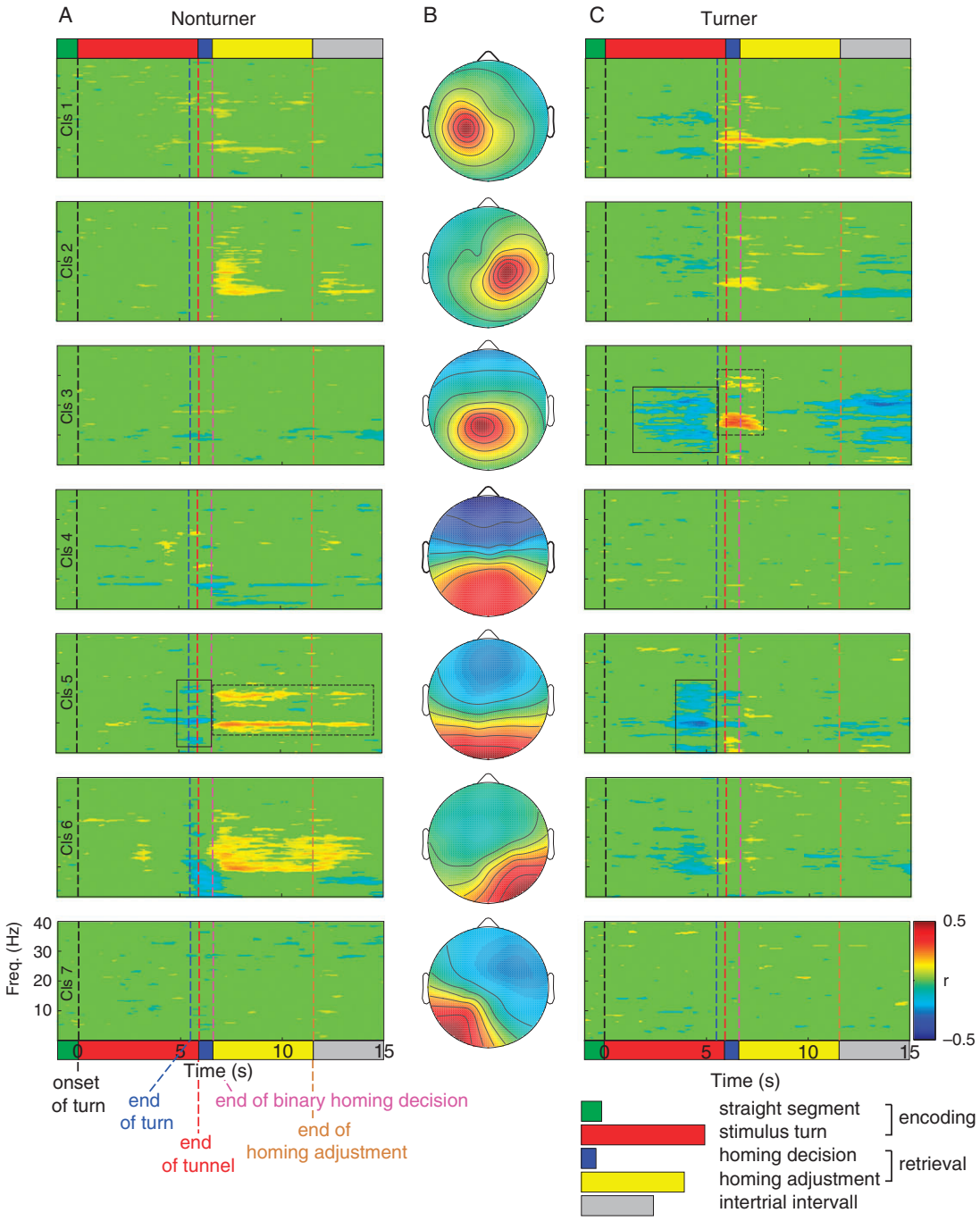

Figure 6. Correlation coefficients computed between event-related spectral perturbations (ERSP) and homing errors for selected clusters. (A) Nonturners' correlation of ERSPs with homing adjustment for selected clusters (as described in Figure 3). (B) Middle column shows selected cluster centroid topographic images (as in Figure 3). (C) Right column displays correlation coefficients for Turners during tunnel passages (same clusters as described for Nonturners). Solid black outlines and broken black outlines indicate significant positive and negative correlation coefficients, respectively, as discussed in the text.

the bilateral inferior (Cls 1 and 2) and central superior parietal cortex (Cls 3) that directly reflected their later homing adjustments. This further supports the important role of the parietal cortex in computing and maintaining egocentric spatial representations. In addition, Turners demonstrated significant power increases in the alpha band in a cluster with a location of the cluster centroid approximating the dorsal retrosplenial cortex (Cls 5). These power increases were negatively correlated with Turners' homing adjustments and signed errors. This supports the involvement of retrosplenial cortex for spatial navigation. While the involvement of an additional, more ventrally located, retrosplenial cluster points to a possible dissociation of distinct regions in the posterior cingulate cortex (Vogt, Vogt, & Laureys, 2006), further studies have to investigate the role of these regions in spatial navigation. Importantly, the retrosplenial cortex is a key structure of a network supporting navigation (Gramann, in press;

Vann, Aggleton, & Maguire, 2009), and our results support its important role in both allocentric and egocentric navigation.

Updating of Turners' cognitive heading was accompanied by strong alpha suppression in or near the superior and bilateral inferior parietal cortex and in or near the retrosplenial cortex. While the parietal alpha (and first harmonic frequency band) desynchronization extended over most of the turning segment, an augmentation of the same frequencies in the retrosplenial cortex was confined to the second half of the stimulus turn. This indicates that the parietal cortex might be necessary for the computation and maintenance of heading changes based on an egocentric reference frame very early in the time course of computing deviations from the reference direction (first straight segment). In contrast, the late onset of retrosplenial alpha modulation indicates that this cortical structure is involved in subsequent stages of processing (Gramann et al., 2010). Such processes might be associated with establishing new heading directions for the future path or, more generally, the translation of egocentric heading information into an allocentric reference frame (Byrne, Becker, & Burgess, 2007; Gramann, in press; Maguire, 2001; Vann et al., 2009).

During the encoding phase, parietal alpha suppression was present in both strategy groups. However, while this power suppression was significantly correlated with Turners' homing adjustment (and relative error), Nonturners revealed no such covariation. Alpha suppression, or event-related desynchronization (ERD), could be interpreted as activation of the respective cortical area (Pfurtscheller, Stancak, & Neuper, 1996). Both strategy groups processed the same visual flow information from an egocentric perspective and, consequently, the parietal cortex was actively processing spatial information from a first-person perspective in both groups. The difference between the strategy groups was not related to the processing of egocentric spatial information as indicated in comparable parietal alpha power modulation. Rather, the strategy groups differed in how they used the output of the spatial computation that was associated with the specific alpha suppression. Only Turners demonstrated a linear relationship of parietal alpha suppression with homing adjustments further emphasizing the central role of the parietal cortex in egocentric navigation.

Spectral Modulations during Retrieval of Spatial Information

Nonturners, using an allocentric reference frame, demonstrated a linear relationship of alpha power and homing adjustments towards the end of navigation only in or near the dorsal retrosplenial cortex (Cls 5). Additional significant correlations were observed after navigating the tunnel passages, i.e., during the binary homing decision and the subsequent adjustment of the homing arrow. Nonturners showed stronger alpha suppression in or near lateral occipital (Cls 6 and 7) areas as compared to Turners, and this activation correlated with homing arrow adjustments. Nonturners showed stronger alpha suppression in or near the retrosplenial cortex during homing angle adjustments. This task-related alpha suppression in the occipital and retrosplenial cortex may not only reflect increased demands on visuo-attentional processing but also the process of retrieving information based on an allocentric reference frame (Byrne et al, 2007).

Besides the strong modulation of alpha power in several brain regions, we found theta activity to be strongly synchronized especially during the binary homing decision. Kahana and colleagues (Kahana et al., 1999) studied human brain dynamics during virtual maze navigation by intracortical EEG (iEEG) demonstrating increased theta power during more complex mazes and during recall of maze layout. Similar results were found during maze navigation using EEG (Bischof & Boulanger, 2003; Nishiyama, Mizuhara, Miwakeichi, & Yamaguchi, 2002). In these studies, wide-spread theta activity was observed with a focus in the parietal and occipital regions during exploration of and way-finding in virtual city environments, supporting its role in sensorimotor integration and spatial learning (Caplan et al., 2001). In the present study a significant augmentation of parietal and occipital theta band power was observed during the primary homing decision, possibly reflecting a more general process associated with spatial decisions (Bischof & Boulanger, 2003) and the retrieval of a spatial representation (Jacobs, Hwang, Curran, & Kahana, 2006).

In conclusion, the results of the present investigation support the assumption that during navigation of virtual tunnels devoid of any landmarks, distinct spatial representations are active, and the majority of participants revealed a stable proclivity to adjust a homing arrow based on only one reference frame. However, three participants could not be categorized as Turner or Nonturner based on their homing adjustments. It remains an open question whether these participants lost orientation on a subset of trials or whether they belong to a subgroup of participants flexibly using different reference frames (Gramann in press; Gramann, Wing, Jung, Virre, & Riecke, unpublished manuscript). For all participants further investigated, Turners and Nonturners shared similar spectral perturbation patterns during the task. A strong alpha modulation was observed in or near parietal, occipital, and retrosplenial cortices for both strategy groups. This supports the assumption that all participants computed information based on an egocentric and an allocentric reference frame in parallel even though different cortical structures are likely to be used in a dominant fashion based on the preferred reference frame (Gramann, in press; Gramann et al., 2005, 2006, 2010). However, power modulation of the alpha band in parietal cortex correlated with homing arrow adjustments only for participants using an egocentric reference frame. Besides providing additional support to the central role of the parietal cortex in computing and maintaining spatial information based on an egocentric reference frame, this result implies that only Turners use egocentrically represented spatial information to respond to the homing task. Importantly, Nonturners also revealed significant power decreases in the parietal cortex during encoding of spatial information. However, these modulations did not covary with their homing adjustments, indicative of the use of a different reference frame for responding as compared to the reference frame for encoding. In contrast, for Nonturners, modulation of alpha power in or near occipital and retrosplenial cortex was observed *after* navigation and with onset of the binary homing decision and the adjustment of the homing response. If activity in retrosplenial cortex is reflected in a desynchronization in the alpha band (as is the case for occipital and parietal cortex), then the observed pattern of alpha decrease in occipital and retrosplenial cortex might reflect retrieval of allocentrically coded spatial information from the retrosplenial (and probably the medio-temporal) cortex and visual imagery of this allocentrically represented information in occipital cortex. This *post hoc* explanation is appealing because of its fit with existing models (e.g., Byrne et al., 2007) but has to be investigated in future studies.

In summary, the differences in spectral modulation in distinct brain areas and at distinct time points of spatial information processing support the important role of parallel reference frame computations during spatial navigation. Core areas subserving the computation of egocentric and allocentric reference frames comprise, among others, the parietal and retrosplenial cortex, respectively. Navigators compute and maintain spatial relations embedded in distinct reference frames but preferentially choose specific frames for solving spatial tasks. The use of advanced analyses methods based on EEG data in the future might allow for predicting spatial awareness of participants when their proclivity to use one or the other reference frame is considered.

References

Bischof, W. F., & Boulanger, P. (2003). Spatial navigation in virtual reality environments: An EEG analysis. *Cyberpsychology, Behavior, and Social Networking*, *6*, 487–495.

Buzsaki, G. (2005). Theta rhythm of navigation: Link between path integration and landmark navigation, episodic and semantic memory. *Hippocampus*, *15*, 827–840. doi: 10.1002/Hipo.20113.

Byrne, P., Becker, S., & Burgess, N. (2007). Remembering the past and imagining the future: A neural model of spatial memory and imagery. *Psychological Review*, *114*, 340–375.

Caplan, J. B., Madsen, J. R., Raghavachari, S., & Kahana, M. J. (2001). Distinct patterns of brain oscillations underlie two basic parameters of human maze learning. *Journal of Neurophysiology*, *86*, 368–380.

Caplan, J. B., Madsen, J. R., Schulze-Bonhage, A., Aschenbrenner-Scheibe, R., Newman, E. L., & Kahana, M. J. (2003). Human theta oscillations related to sensorimotor integration and spatial learning. *Journal of Neuroscience*, *23*, 4726–4736.

Chen, Y., Duann, J., Chuang, S., Lin, C., Ko, L., Jung, T., & Lin, C. (2010). Spatial and temporal EEG dynamics of motion sickness. *Neuroimage*, *49*, 2862–2870.

Committeri, G., Galati, G., Paradis, A. L., Pizzamiglio, L., Berthoz, A., & LeBihan, D. (2004). Reference frames for spatial cognition: Different brain areas are involved in viewer-, object-, and landmark-centered judgments about object location. *Journal of Cognitive Neuroscience*, *16*, 1517–1535.

Delorme, A., & Makeig, S. (2004). EEGLAB: An open source toolbox for analysis of single-trial EEG dynamics including independent component analysis. *Journal of Neuroscience Methods*, *134*, 9–21.

Doeller, C. F., Barry, C., & Burgess, N. (2010). Evidence for grid cells in a human memory network. *Nature*, *463*, 657–661. doi: nature08704 [pii]10.1038/nature08704.

Ekstrom, A. D., Caplan, J. B., Ho, E., Shattuck, K., Fried, I., & Kahana, M. J. (2005). Human hippocampal theta activity during virtual navigation. *Hippocampus*, *15*, 881–889.

Ekstrom, A. D., Kahana, M. J., Caplan, J. B., Fields, T. A., Isham, E. A., Newman, E. L., & Fried, I. (2003). Cellular networks underlying human spatial navigation. *Nature*, *425*, 184–188.

Fink, G. R., Marshall, J. C., Weiss, P. H., Stephan, T., Grefkes, C., Shah, N. J., . . . Dieterich, M. (2003). Performing allocentric visuospatial judgments with induced distortion of the egocentric reference frame: An fMRI study with clinical implications. *Neuroimage*, *20*, 1505–1517. doi: 10.1016/J.Neuroimage.2003.07.006.

Galati, G., Lobel, E., Vallar, G., Berthoz, A., Pizzamiglio, L., & Le Bihan, D. (2000). The neural basis of egocentric and allocentric coding of space in humans: A functional magnetic resonance study. *Experimental Brain Research*, *133*, 156–164.

Gilbert, P. E., Kesner, R. P., & DeCoteau, W. E. (1998). Memory for spatial location: Role of the hippocampus in mediating spatial pattern separation. *Journal of Neuroscience*, *18*, 804–810.

Gramann, K. (in press). Embodiment of spatial reference frames and individual differences in reference frame proclivity. [Review]. *Spatial Cognition and Computation*.

Gramann, K., El Sharkawy, J., & Deubel, H. (2009). Eye-movements during navigation in a virtual tunnel. *International Journal of Neuroscience*, *119*, 1755–1778. doi: 10.1080/00207450903170361.

Gramann, K., Muller, H. J., Eick, E. M., & Schonebeck, B. (2005). Evidence of separable spatial representations in a virtual navigation task. *Journal of Experimental Psychology-Human Perception and Performance*, *31*, 1199–1223. doi: 10.1037/0096-1523.31.6.1199.

Gramann, K., Muller, H. J., Schonebeck, B., & Debus, G. (2006). The neural basis of ego- and allocentric reference frames in spatial navigation: Evidence from spatio-temporal coupled current density reconstruction. *Brain Research*, *1118*, 116–129. doi: 10.1016/J.Brainres.2006.08.005.

Gramann, K., Onton, J., Riccobon, D., Mueller, H. J., Bardins, S., & Makeig, S. (2010). Human brain dynamics accompanying use of egocentric and allocentric reference frames during navigation. *Journal of Cognitive Neuroscience*, *22*, 2836–2849.

Gramann, K., Wing, S., Jung, T.-P., Virre, E., & Riecke, B. E. Switching spatial reference frames for yaw and pitch navigation. In preparation.

Gron, G., Wunderlich, A. P., Spitzer, M., Tomczak, R., & Riepe, M. W. (2000). Brain activation during human navigation: Gender-different neural networks as substrate of performance. *Nature Neuroscience*, *3*, 404–408.

Gwin, J. T., Gramann, K., Makeig, S., & Ferris, D. P. (2010). Removal of movement artifact from high-density EEG recorded during walking and running. *Journal of Neurophysiology*, *103*, 3526–3534. doi: 10.1152/Jn.00105.2010.

Hsu, C. F., Lin, C. T., Huang, T. Y., & Young, K. Y. (2005). Development of multipurpose virtual-reality dynamic simulator with force-reflection joystick. *Proceedings of the Institution of Mechanical Engineers Part I—Journal of Systems and Control Engineering*, *219*, 187–195.

Jacobs, J., Hwang, G., Curran, T., & Kahana, M. J. (2006). EEG oscillations and recognition memory: Theta correlates of memory retrieval and decision making. *Neuroimage*, *32*, 978–987. doi: 10.1016/J.Neuroimage.2006.02.018.

Jordan, K., Schadow, J., Wuestenberg, T., Heinze, H. J., & Jancke, L. (2004). Different cortical activations for subjects using allocentric or egocentric strategies in a virtual navigation task. *Neuroreport*, *15*, 135–140. doi: 10.1097/01.Wnr.0000097043.56589.B6.

Jung, T. P., Makeig, S., Humphries, C., Lee, T. W., McKeown, M. J., Iragui, V., & Sejnowski, T. J. (2000). Removing electroencephalographic artifacts by blind source separation. *Psychophysiology*, *37*, 163–178.

Jung, T. P., Makeig, S., Westerfield, M., Townsend, J., Courchesne, E., & Sejnowski, T. J. (2001). Analysis and visualization of single-trial event-related potentials. *Human Brain Mapping*, *14*, 166–185.

Kahana, M. J., Sekuler, R., Caplan, J. B., Kirschen, M., & Madsen, J. R. (1999). Human theta oscillations exhibit task dependence during virtual maze navigation. *Nature*, *399*, 781–784.

Karnath, H. O. (1997). Spatial orientation and the representation of space with parietal lobe lesions. *Philosophical Transactions of the Royal Society of London Series B—Biological Sciences*, *352*, 1411–1419.

Klatzky, R. L. (1998). *Allocentric and egocentric spatial representations: Definitions, distinctions, and interconnections* (Vol. 1). New York, NY: Springer.

Lee, T. W., Girolami, M., & Sejnowski, T. J. (1999). Independent component analysis using an extended infomax algorithm for mixed subgaussian and supergaussian sources. *Neural Computation*, *11*, 417–441.

Lin, C. T., Yang, F. S., Chiou, T. C., Ko, L. W., Duann, J. R., & Gramann, K. (2009). *EEG-based spatial navigation estimation in a virtual reality driving environment*. Proceedings of the Ninth IEEE International Conference on Bioinformatics and Bioengineering. Taichung, Taiwan, 435–438.

Loomis, J., Klatzky, R., Golledge, R. G., & Philbeck, J. W. (1999). Human navigation by path integration. In R. G. Golledge (Ed.), *Wayfinding behavior: Cognitive mapping and other spatial processes* (pp. 125–151). Baltimore, MD: Johns Hopkins University Press.

Maguire, E. A. (1997). Hippocampal involvement in human topographical memory: Evidence from functional imaging. *Philosophical Transactions of the Royal Society of Lond Series B—Biological Sciences*, *352*, 1475–1480.

Maguire, E. A. (2001). The retrosplenial contribution to human navigation: A review of lesion and neuroimaging findings. *Scandinavian Journal of Psychology*, *42*, 225–238.

Maguire, E. A., Burgess, N., Donnett, J. G., Frackowiak, R. S., Frith, C. D., & O'Keefe, J. (1998). Knowing where and getting there: A human navigation network. *Science*, *280*, 921–924.

Maguire, E. A., Nannery, R., & Spiers, H. J. (2006). Navigation around London by a taxi driver with bilateral hippocampal lesions. *Brain*, *129*, 2894–2907.

Makeig, S. (1993). Auditory event-related dynamics of the EEG spectrum and effects of exposure to noise. *Electroencephalography and Clinical Neurophysiology*, *86*, 283–293.

Makeig, S., Debener, S., Onton, J., & Delorme, A. (2004). Mining event-related brain dynamics. *Trends in Cognitive Sciences*, *8*, 204–210. doi: 10.1016/j.tics.2004.03.008 S1364661304000816 [pii].

Makeig, S., Gramann, K., Jung, T. P., Sejnowski, T. J., & Poizner, H. (2009). Linking brain, mind and behavior. *International Journal of Psychophysiology*, *73*, 95–100. doi: 10.1016/J.Ijpsycho.2008.11.008.

Makeig, S., Jung, T. P., Bell, A. J., Ghahremani, D., & Sejnowski, T. J. (1997). Blind separation of auditory event-related brain responses into independent components. *Proceedings of the National Academy of Sciences U S A*, *94*, 10979–10984.

Makeig, S., Westerfield, M., Jung, T. P., Enghoff, S., Townsend, J., Courchesne, E., & Sejnowski, T. J. (2002). Dynamic brain sources of visual evoked responses. *Science*, *295*, 690–694.

Mellet, E., Bricogne, S., Tzourio-Mazoyer, N., Ghaem, O., Petit, L., Zago, L., ... Denis, M. (2000). Neural correlates of topographic mental exploration: The impact of route versus survey perspective learning. *Neuroimage*, *12*, 588–600. doi: 10.1006/Nimg.2000.0648.

Moscovitch, M., Nadel, L., Winocur, G., Gilboa, A., & Rosenbaum, R. S. (2006). The cognitive neuroscience of remote episodic, semantic and spatial memory. *Current Opinion in Neurobiology*, *16*, 179–190. doi: 10.1016/J.Conb.2006.03.013.

Moscovitch, M., Rosenbaum, R. S., Gilboa, A., Addis, D. R., Westmacott, R., Grady, C., ... Nadel, L. (2005). Functional neuroanatomy of remote episodic, semantic and spatial memory: A unified account based on multiple trace theory. *Journal of Anatomy*, *207*, 35–66.

Nishiyama, N., Mizuhara, H., Miwakeichi, F., & Yamaguchi, Y. (2002). *Theta episodes observed in human scalp EEG during virtual navigation-spatial distribution and task dependence*. Paper presented at the Proceeding of the 9th International Conference on Neural Information Processing. Singapore.

O'Keefe, J., & Dostrovsky, J. (1971). The hippocampus as a spatial map. Preliminary evidence from unit activity in the freely-moving rat. *Brain Research*, *34*, 171–175. doi: 0006-8993(71)90358-1 [pii].

Onton, J., Westerfield, M., Townsend, J., & Makeig, S. (2006). Imaging human EEG dynamics using independent component analysis. *Neuroscience and Biobehavioral Reviews*, *30*, 808–822. doi: S0149-7634(06)00050-9 [pii] 10.1016/j.neubiorev.2006.06.007.

Oostenveld, R., & Oostendorp, T. F. (2002). Validating the boundary element method for forward and inverse EEG computations in the presence of a hole in the skull. *Human Brain Mapping*, *17*, 179–192.

Peuskens, H., Sunaert, S., Dupont, P., Van Hecke, P., & Orban, G. A. (2001). Human brain regions involved in heading estimation. *Journal of Neuroscience*, *21*, 2451–2461.

Pfurtscheller, G., Stancak, A., & Neuper, C. (1996). Event-related synchronization (ERS) in the alpha band—An electrophysiological correlate of cortical idling: A review. *International Journal of Psychophysiology*, *24*, 39–46.

Plank, M., Müller, H., Onton, J., Makeig, S., & Gramann, K. (2010). Human EEG Correlates of spatial navigation within egocentric and allocentric reference frames. In C. Hölscher, T. Shipley, M. Olivetti Belardinelli, J. Bateman, & N. Newcombe (Eds.), *Spatial cognition VII* (Vol. 6222, pp. 191–206). Heidelberg, Germany: Springer Berlin.

Raghavachari, S., Kahana, M. J., Rizzuto, D. S., Caplan, J. B., Kirschen, M. P., Bourgeois, B., ... Lisman, J. E. (2001). Gating of human theta oscillations by a working memory task. *Journal of Neuroscience*, *21*, 3175–3183.

Rosenbaum, R. S., Priselac, S., Kohler, S., Black, S. E., Gao, F. Q., Nadel, L., & Moscovitch, M. (2000). Remote spatial memory in an amnesic person with extensive bilateral hippocampal lesions. *Nature Neuroscience*, *3*, 1044–1048.

Sdoia, S., Couyoumdjian, A., & Ferlazzo, F. (2004). Opposite visual field asymmetries for egocentric and allocentric spatial judgments. *Neuroreport*, *15*, 1303–1305. doi: 10.1097/01.Wnr.0000125776.27645.C4.

Seubert, J., Humphreys, G. W., Muller, H. J., & Gramann, K. (2008). Straight after the turn: The role of the parietal lobes in egocentric space processing. *Neurocase*, *14*, 204–219. doi: 10.1080/13554790802108398.

Shelton, A. L., & Gabrieli, J. D. (2002). Neural correlates of encoding space from route and survey perspectives. *Journal of Neuroscience*, *22*, 2711–2717.

Thut, G., Nietzel, A., & Pascual-Leone, A. (2005). Dorsal posterior parietal rTMS affects voluntary orienting of visuospatial attention. *Cerebral Cortex*, *15*, 628–638. doi: 10.1093/Cercor/Bhh164.

Vallar, G., Lobel, E., Galati, G., Berthoz, A., Pizzamiglio, L., & Le Bihan, D. (1999). A fronto-parietal system for computing the egocentric spatial frame of reference in humans. *Experimental Brain Research*, *124*, 281–286.

Vann, S. D., Aggleton, J. P., & Maguire, E. A. (2009). What does the retrosplenial cortex do? *Nature Reviews Neuroscience*, *10*, 792–U750. doi: 10.1038/Nrn2733.

Vogt, B. A., Vogt, L., & Laureys, S. (2006). Cytology and functionally correlated circuits of human posterior cingulate areas. *Neuroimage*, *29*, 452–466. doi: 10.1016/J.Neuroimage.2005.07.048.

Zaehle, T., Jordan, K., Wustenberg, T., Baudewig, J., Dechent, P., & Mast, F. W. (2007). The neural basis of the egocentric and allocentric spatial frame of reference. *Brain Research*, *1137*, 92–103. doi: 10.1016/J.Brainres.2006.12.044.

(Received March 30, 2011; Accepted June 15, 2011)